



HAL
open science

Inhibition of type 1 fimbriae-mediated Escherichia coli adhesion and biofilm formation by trimeric cluster thiomannosides conjugated to diamond nanoparticles.

Manakamana Khanal, Fanny Larsonneur, Victoriia Raks, Alexandre Barras, Jean-Sebastien Baumann, Fernando Ariel Martin, Rabah Boukherroub, Jean-Marc Ghigo, Carmen Ortiz Mellet, Vladimir Zaitsev, et al.

► To cite this version:

Manakamana Khanal, Fanny Larsonneur, Victoriia Raks, Alexandre Barras, Jean-Sebastien Baumann, et al.. Inhibition of type 1 fimbriae-mediated Escherichia coli adhesion and biofilm formation by trimeric cluster thiomannosides conjugated to diamond nanoparticles.. *Nanoscale*, 2015, 7 (6), pp.2325–2335. 10.1039/c4nr05906a . pasteur-01378734

HAL Id: pasteur-01378734

<https://pasteur.hal.science/pasteur-01378734v1>

Submitted on 17 Nov 2016

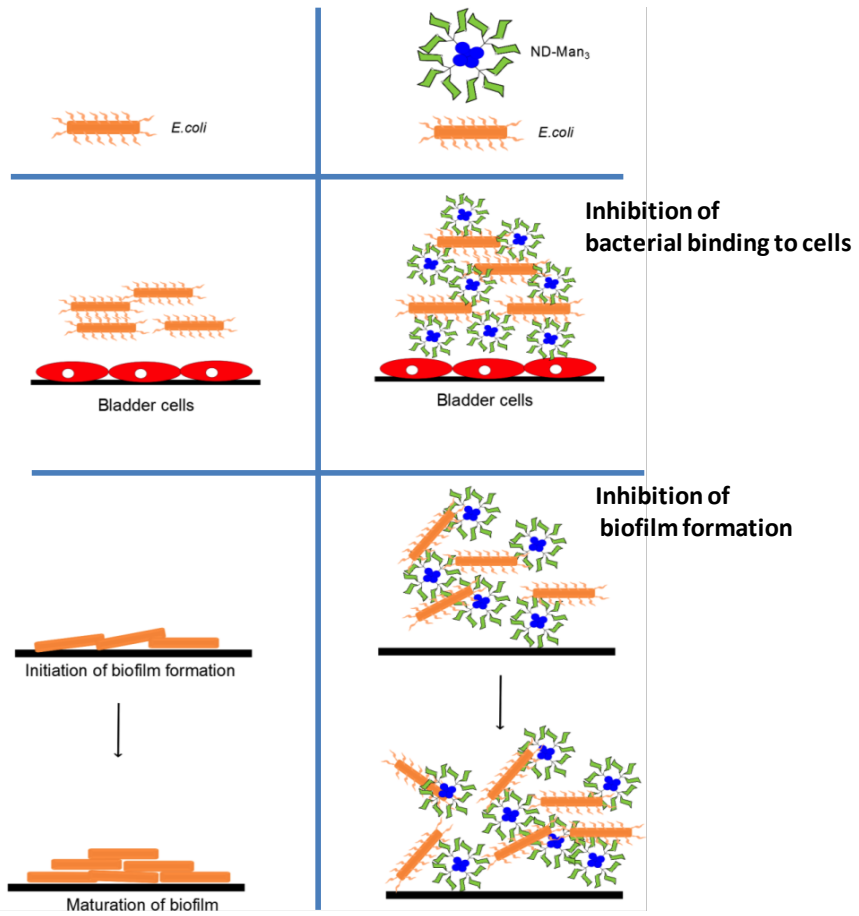
HAL is a multi-disciplinary open access archive for the deposit and dissemination of scientific research documents, whether they are published or not. The documents may come from teaching and research institutions in France or abroad, or from public or private research centers.

L'archive ouverte pluridisciplinaire **HAL**, est destinée au dépôt et à la diffusion de documents scientifiques de niveau recherche, publiés ou non, émanant des établissements d'enseignement et de recherche français ou étrangers, des laboratoires publics ou privés.



Distributed under a Creative Commons Attribution - NonCommercial - ShareAlike 4.0 International License

TOC image



**Inhibition of type 1 fimbriae-mediated *Escherichia coli* adhesion and biofilm formation
by trimeric cluster thiomannosides conjugated to diamond nanoparticles**

Manakamana Khanal,^{a, #} Fanny Larssonneur,^{b, c, #} Victoriia Raks,^{d, e} Alexandre Barras,^a Jean-Sébastien Baumann,^f Fernando Ariel Martin,^b Rabah Boukherroub,^a Jean-Marc Ghigo,^b Carmen Ortiz Mellet,^e Vladimir Zaitsev,^{e, g} Jose M. Garcia Fernandez,^h Christophe Beloin,^{b, *} Aloysius Siriwardena,^{f, *} Sabine Szunerits,^{a, *}

^a *Institut de Recherche Interdisciplinaire (IRI, USR CNRS 3078), Université Lille 1, Parc de la Haute Borne, 50 Avenue de Halley, BP 70478, 59658 Villeneuve d'Ascq, France.*

^b *Institut Pasteur, Unité de Génétique des Biofilms, 28 rue du Dr. Roux, 75724 Paris cedex 15, France.*

^c *Université Paris Diderot, Ecole Doctorale Bio Sorbonne Paris Cité (BioSPC), Cellule Pasteur, rue du Dr. Roux, 75724 Paris cedex 15, France.*

^d *Taras Shevchenko University, 60 Vladimirska str., Kiev, Ukraine*

^e *Departamento de Química Orgánica, Facultad de Química, Universidad de Sevilla, c/ Profesor García González, 41012 Sevilla, Spain.*

^f *Laboratoire de Glycochimie des Antimicrobiens et des Agroressources (FRE 3517 CNRS), Université de Picardie Jules Vernes, 33 Rue St Leu, 80039 Amiens, France.*

^g *Chemistry Department, Pontifical Catholic University of Rio de Janeiro, Rua Marques de Sao Vicente, 225-Gavea, Rio de Janeiro, 22451-900, Brazil*

^h *Investigaciones Químicas (IIQ), CSIC – Universidad de Sevilla, Avda. Américo Vespucio 49, 41092 Sevilla, Spain*

Keywords: diamond nanoparticles, glycoclusters, anti-adhesives, *E. coli*, FimH, biofilm

[#] these authors contributed equally to the work

^{*} to whom correspondence should be sent: cbeloin@pasteur.fr; aloyusius.siriwardena@u-picardie.fr; Sabine.Szunerits@iri.univ-lille1.fr;

Abstract:

Recent advances in nanotechnology have seen the development of a number of microbiocidal and/or anti-adhesive nanoparticles displaying activity against biofilms. In this work, trimeric thiomannoside clusters conjugated to nanodiamond particles (ND) were targeted for investigation. NDs have attracted attention as a biocompatible nanomaterial and we were curious to see whether the high mannose glycotope density obtained upon grouping monosaccharide units in triads might lead to the corresponding ND-conjugates behaving as effective inhibitors of *E. coli* type 1 fimbriae-mediated adhesion as well as of biofilm formation. The required trimeric thiosugar clusters were obtained through a convenient thiol-ene “click” strategy and were subsequently conjugated to alkynyl-functionalized NDs using a Cu(I)-catalysed “click” reaction. We demonstrated that the tri-thiomannoside cluster-conjugated NDs (ND-Man₃) show potent inhibition of type 1 fimbriae-mediated *E. coli* adhesion to yeast and T24 bladder cells as well as of biofilm formation. The biofilm disrupting effects demonstrated here have only rarely been reported in the past for analogues featuring such simple glycosidic motifs. Moreover, the finding that the tri-thiomannoside cluster (Man₃N₃) is itself a relatively efficient inhibitor, even when not conjugated to any ND edifice, suggests that alternative mono- or multivalent sugar-derived analogues might also be usefully explored for *E. coli*-mediated biofilm disrupting properties.

1. INTRODUCTION

Bacterial infectious diseases pose a major threat to human health. Several share clinical characteristics such as chronic inflammation and tissue damage, and are greatly exacerbated when microorganisms grow as biofilms on mucosal surfaces or medical devices.^{1,2} Biofilms enable the bacteria residing within them to counter and resist the action of the human immune system and to enhance their tolerance towards antibiotics, leading to infections that are very difficult to eradicate.³⁻⁵ The threat of biofilm-related infections has been greatly aggravated with the emergence of multidrug resistant bacteria, a phenomenon that has been compounded in the past decades with the overuse and misuse of antibiotics. These and other considerations have generated an increased interest in the development of non-biocidal anti-infective strategies as alternatives to antibiotics, as these would be expected to show reduced tendency to provoke the appearance of resistant strains.⁶⁻¹³ One such approach is the development of a number of microbiocidal and/or anti-adhesive nanoparticles displaying activity against biofilms.¹⁴⁻¹⁹ Among the targets that have been identified for anti-adhesive nanoparticles are type 1 fimbriae, which constitute major virulence factors produced by *Escherichia coli* (*E. coli*).²⁰ Type 1 fimbriae are filamentous tubular structures each of 0.2-2.0 μm in length and 5-7 nm in diameter that are distributed over the entire surface of the bacterium.²¹ In various *E. coli* strains the lectin located at the extremity of type 1 fimbriae, FimH, contributes to tissue colonization through its specific recognition of the terminal α -D-mannopyranosyl units present on cell-surface glycoproteins. FimH-mediated adhesion to such mannosyl moieties has been demonstrated to be crucial for the interaction of *E. coli* with uroplakins and consequently for bladder colonization.²² Disruption of this interaction has been proposed as a promising strategy for the development of an anti-adhesive therapy.^{23,24}

While a number of multivalent as well as monovalent sugar-based ligands have been reported to show promise as effective inhibitors of *E. coli* adhesion to eukaryotic cells,^{9, 20, 25-31} multivalent presentation of carbohydrate ligands on appropriate scaffolds has been demonstrated, in several instances, to lead to significantly increased affinities for their appropriate lectin target compared to a monovalent references.³²⁻³⁷ These avidities can be dramatically superior to those arising from a simple additive effect. The types of multivalent structures targeting FimH thus far reported are very varied and range from small- to medium-sized scaffolds presenting carbohydrate-derived ligands, to larger entities such as sugar-decorated polymers and nanoparticles, and a multitude of creatively designed compounds in between.^{20, 38, 39}

We and others have been interested in exploring whether the reported characteristic properties of nanodiamonds (NDs) might be taken advantage of in the development of useful inhibitors of type 1 fimbriae-mediated *E. coli* adhesion.⁴⁰⁻⁴² ND particles are completely inert, optically transparent, biocompatible and moreover, easily functionalizable *via* a variety of strategies depending on their intended application.⁴³⁻⁵⁰ Although their *in vivo* toxicity depends in particular on their surface characteristics (as well as the nature of the ligands they carry on their surface),⁵¹ ND particles have thus far been reported not to induce significant cytotoxicity in a variety of cell types.⁵¹⁻⁵⁴ The demonstration that our 1st-generation sugar-conjugated NDs do show marked anti-adhesive activity in cell-based assays without displaying toxicity against eukaryotic cells comforted us in our choice of particle and convinced us that sugar-NDs should indeed be further pursued as biomaterials. Particularly striking was the unexpected observation that these ND-mannose conjugates are able to inhibit *E. coli*-induced biofilm formation. Such a feature has indeed only been observed rarely for ligands of FimH but would be expected to constitute a very desirable additional attribute in any potential anti-adhesive molecule.^{9, 40, 55} Moreover, anti-biofilm disrupting activity had not apparently been described previously for alternative glyco-nanoparticles (glyco-NPs) such as glycofullerenes, gold-based glyco-NPs or for other multivalent mannose-derived molecules.^{33, 36, 41}

The coupling strategy used for the fabrication of our 1st-generation glyco-NDs was selected with the expectation that it would ensure not only a convenient means of conjugating carbohydrate moieties to the ND core, but also provide a linker that would itself constitute an extended ligand for FimH. In that approach propargyl sugar derivatives were ligated using a Cu(I)-catalysed Huisgen cycloaddition reaction (“click” reaction) to NDs decorated with surface azidophenyl functions. To further scrutinize the origin of the bacterial adhesion and biofilm growth inhibition activities observed for our 1st-generation glyco-NDs, we embarked on the investigation of a second, structurally complimentary, family of sugar-conjugated NDs. It was decided that the 2nd-generation ND-sugar conjugates were to be obtained through an alternative sugar-conjugation strategy and, in addition, would feature a trimeric thiomannoside cluster motif as a contrasting mode of surface-sugar presentation. Indeed various *O*-glycoside-derived trimeric clusters have been shown to be strong ligands for FimH compared with their corresponding monovalent analogues.^{20, 28} Moreover, it has been demonstrated that trimeric mannoside and thiomannoside clusters, related to those proposed, often give relatively large multivalent effects towards mannose-specific lectins.⁵⁶⁻⁶⁰ The sugar-linker of our 2nd-generation ND-sugar conjugates is quite different from the one

featured in the 1st-generation NDs, (synthesized through the “clicking” of propargyl glycosides to ND-grafted azido functions) and would thus very probably make different secondary interactions with the sugar-binding pocket in FimH. Furthermore, the trimeric thiosugar cluster backbone would be expected to be relatively flexible and, in addition, its peripheral thiomannosyl moieties held much further away from the ND surface than the mannosyl units featured in the 1st-generation NDs. Taken together, we suspected that all these factors would serve to render the sugar moieties present in the targeted 2nd-generation ND-conjugates more accessible to FimH receptors on the bacterial surface than those featured in our 1st-generation conjugates and thus give contrasting behavior in the projected biological assays.

An additional feature of the second family of glyco-NDs proposed in this work is the installation of thioglycoside linkages which would render the anomeric tethering function much more robust to acidic or enzymatic hydrolysis than the *O*-glycosidic functions featured in our initial ND-sugar conjugates. This strategy has been a design feature of a multitude of thioglycoside-based ligands⁶¹ and we were surprised to discover that such a functional group motif had rarely been integrated into potential inhibitors of FimH and FimH-mediated *E. coli* adhesion events. Yet another difference between the 1st- and targeted 2nd-generation sugar-NDs is that the concentration of surface triazole functions relative to that of conjugated mannosyl moieties in the later family would be much lower than in the original ND sugar-conjugates. We were curious to ascertain if inhibition of type 1 fimbriae-mediated adhesion might in some way be connected to: (i) the presence and accessibility of surface triazole functions; (ii) to the presence of multiple surface-conjugated mannosyl units; (iii) to the inherent physico-chemical characteristics of the ND core itself, or even to some combination of the three.

We show in this paper the successful integration of trimeric thiomannosyl clusters onto alkynyl-terminated NDs, to give the targeted 2nd-generation sugar-conjugated NDs (ND-Man₃) (**Figure 1**). Thiolactoside trimer-ND conjugates (ND-Lac₃) and ND-OH particles have also been prepared as negative controls. These compounds have all been tested as inhibitors of *E. coli* adhesion to yeast and also to T24 bladder cells. The thiomannosyl trimer-NDs (ND-Man₃), but not the negative controls, have been found to be strong inhibitors of both *E. coli* adhesions in both assays. In addition, these ND-Man₃ particles are shown also to inhibit *E. coli*-driven biofilm growth significantly.

2. EXPERIMENTAL

2.1. Materials

Reagents and solvents were purchased from commercial sources and used without further purification. Azo-bis(isobutyronitrile), dichloromethane, trifluoromethanesulfonic anhydride, pyridine, and N,N-dimethylformamide are indicated by the acronyms AIBN, DCM, Tf₂O, Py, and DMF, respectively. Thin-layer chromatography (TLC) was carried out on aluminum sheets coated with Kieselgel 60 F254, with visualization by UV light and by charring with 10% H₂SO₄ or 0.2% ninhydrin. Column chromatography was carried out on silica gel 60 (230–400 mesh).

2.2. Synthesis of tri-thiomannoside (Man₃N₃) and tri-thiolactoside (Lac₃N₃) cluster ligands for ND conjugation

The synthesis of the new trivalent clusters (Man₃N₃) and (Lac₃N₃) (**Figure 2**) was achieved following a four-step reaction sequence involving: (i) radical addition of the corresponding per-*O*-acetyl-1-thiosugar **B** or **C** to tri-*O*-allylpentaerythritol **A**, using either UV (250 nm) light in DCM (for **B**; room temperature, 1 h) or AIBN in dioxane (for **C**; 75 °C, 3 h) as radical initiator; (ii) activation of the focal hydroxyl group in the resulting adducts by triflation with Tf₂O-Py in DCM (-25 °C, 40 min); (iii) nucleophilic displacement of triflate by azide ion by reaction of the crude triflic esters with NaN₃ in DMF (room temperature, 3 h; 73 and 50% yield over three steps for the previously reported per-*O*-acetylated azide-armed trimannoside **D**⁶² and trilactoside **E**,⁶³ respectively); and (iv) final catalytic deacetylation with sodium methylate in dry methanol as detailed below. The precursor triallylated pentaerythritol derivative **A** (**Figure 2**) required for the synthesis of Man₃N₃ and Lac₃N₃ was prepared following the reported procedure.⁶⁴ 2,3,4,6-tetra-*O*-acetyl-1-thio- α -D-mannopyranose (**B**) and 2,3,6,2',3',4',6'-hepta-*O*-acetyl-1-thio- β -lactose (**C**) were prepared from the corresponding sugar per-*O*-acetates in three steps: transformation into the corresponding glycosyl halides, treatment with thiourea, and subsequent hydrolysis of the resulting isothiuronium salt with potassium metabisulfite (K₂S₂O₅) (**Figure 2**).^{65, 66} Full spectral data are reported in supporting material (**Figures S2-S5**).

2,2,2-Tris[5-(α -D-mannopyranosylthio)-2-oxapentyl]ethyl azide (Man₃N₃). To a solution of 2,2,2-tris[5-(2,3,4,6-*O*-tetra-acetyl- α -D-mannopyranosylthio)-2-oxapentyl]ethyl azide (**D**) (294 mg, 0.214 mmol) in dry MeOH (20 mL) was added methanolic MeONa (1 M, 0.1 equiv per mol of acetate). The reaction mixture was stirred at room temperature for 30 min, then

neutralized with Amberlite IRA-120 (H⁺) ion-exchange resin, concentrated, and the resulting residue was freeze-dried to afford Man₃N₃ (189 mg, quant.) as a white solid. [α]_D +154.3 (*c* 0.56, H₂O). *R_f* 0.19 (10:20:1 CH₃CN-H₂O-NH₄OH). ¹H NMR (500 MHz, CD₃OD) δ 5.23 (bs, 3 H, H-1_{Man}), 3.92 (bs, 3 H, H-2_{Man}), 3.89 (ddd, 3 H, *J*_{4,5} = 11.9 Hz, *J*_{5,6b} = 5.6 Hz, *J*_{5,6a} = 2.4 Hz, H-5_{Man}), 3.81 (dd, 3 H, *J*_{6a,6b} = 11.9 Hz, H-6a_{Man}), 3.3 (dd, 3 H, H-6b_{Man}), 3.66 (m, 6 H, H-3_{Man}, H-4_{Man}), 3.51 (t, 6 H, ³*J*_{H,H} = 6.0 Hz, H-3_{Pent}), 3.33 (t, 2 H, ³*J*_{H,H} = 7.0 Hz, CH₂N₃), 3.33 (m, 6 H, H-1_{Pent}), 2.72 (m, 6 H, H-5_{Pent}), 1.88 (m, 6 H, ³*J*_{H,H} = 6.6 Hz, H-4_{Pent}). ¹³C NMR (125.7 MHz, CD₃OD) δ 86.5 (C-1_{Man}), 74.9 (C-5_{Man}), 73.7 (C-2_{Man}), 73.2 (C-3_{Man}), 70.8 (C-3_{Pent}), 70.6 (C-1_{Pent}), 68.9 (C-4_{Man}), 62.7 (C-6_{Man}), 53.1 (CH₂N₃), 44.7 (C_q) 30.8 (C-4_{Pent}), 28.8 (C-5_{Pent}). ESIMS: *m/z* 892.4 [M + Na]⁺. Anal. Calcd for C₃₂H₅₉N₃O₁₈S₃: C, 44.18; H, 6.84; N, 4.83; S, 11.06. Found: C, 43.6; H, 6.66; N, 4.51; S, 10.79.

2,2,2-Tris[5-(β -lactopyranosylthio)-2-oxapentyl]ethyl azide (Lac₃N₃). To a solution of 2,2,2-tris[5-(2,3,6,2',3',4',6'-hepta-*O*-acetyl- β -lactopyranosylthio)-2-oxapentyl]ethyl azide (**E**) (294 mg, 0.131 mmol) in dry MeOH (20 mL) was added methanolic MeONa (1 M, 0.1 equiv per mol of acetate). The reaction mixture was stirred at 40° C for 45 min, then neutralized with Amberlite IRA-120 (H⁺) ion-exchange resin, concentrated, and the resulting residue was freeze-dried to afford Lac₃N₃. (180 mg, quant.) as a white solid. [α]_D -7.4 (*c* 0.60, H₂O). *R_f* 0.17 (6:3:1 CH₃CN-H₂O-NH₄OH). ¹H NMR (500 MHz, D₂O): δ 4.42 (m, 6 H, H-1_{Lact}, H-1'_{Lact}), 4.00-3.30 (m, 54 H, H-2_{Lact} to H-6a,b_{Lact}, H-2'_{Lact} to H-6'a,b_{Lact}, H-1_{Pent}, H-3_{Pent} and CH₂N₃), 2.81 (2 dt, 6 H, *J*_{4',5'} = 7.0 Hz, *J*_{5a',5b'} = 14.0 Hz, H-5_{Pent}), 1.91 (m, 6 H, H-4_{Pent}); ¹³C NMR (125.7 MHz, CD₃OD) δ 105.1 (C-1'_{Lact}), 87.2 (C-1_{Lact}), 80.7 (C-5_{Lact}), 80.5 (C-4_{Lact}), 77.9 (C-3_{Lact}), 77.1 (C-5'_{Lact}), 74.9 (C-3'_{Lact}), 74.1 (C-2_{Lact}), 72.6 (C-2'_{Lact}), 70.9 (C-3_{Pent}), 70.6 (C-1_{Pent}), 70.4 (C-4'_{Lact}), 62.5 (C-6'_{Lact}), 62.3 (C-6_{Lact}), 53.2 (CH₂N₃), 46.8 (C_q), 31.3 (C-4_{Pent}), 28.0 (C-5_{Pent}). ESIMS: *m/z* 1378.4 [M + Na]⁺. Anal. Calcd for C₅₀H₈₉N₃O₃₃S₃: C, 44.27; H, 6.61; N, 3.10; S, 7.09. Found: C, 44.12; H, 6.56; N, 2.87; S, 6.73.

2.3. Tri-thiomannosyl and tri-thiolactosyl cluster conjugation to NDs (respectively, ND-Man₃ and ND-Lac₃)

4-Pentynoic acid (0.20 mmol), DCC (0.22 mmol) and DMAP (0.066 mmol) were dissolved in 5 mL anhydrous DMF. A suspension of ND-OH particles in anhydrous DMF (10 mg in 5 mL) was added and the mixture stirred at room temperature for 24 h under nitrogen. The

alkynyl-terminated ND particles (ND-alkynyl) were isolated through consecutive wash/centrifugation cycles at 12 300 rcf with DMF (twice) and ethanol (twice) and finally oven-dried at 50 °C overnight.

The ND-alkynyl (15 mg) were dispersed in 15 mL of anhydrous DMF and sonicated for 40 min. The “click” reaction was carried out by addition of either Man_3N_3 (4 mM) or Lac_3N_3 and $\text{CuI}(\text{PPh}_3)$ (0.4 mM) to an ND-alkynyl suspension, followed by stirring of both mixtures for 48 h at 80 °C. The resulting reaction mixtures were each separated by centrifugation at 12.300 rcf, purified through consecutive wash/centrifugation cycles at 12 300 rcf with DMF (twice) and 1 mM EDTA water solution (twice), and finally oven-dried at 50 °C overnight.

2.4. Determination of the carbohydrate loading on particles:

A calibration curve was established as described previously.⁴⁰ An aqueous phenol solution (5 wt%, 60 μL) and concentrated H_2SO_4 (900 μL) was added to an aqueous carbohydrate solution (60 μL), the mixture was stirred for 10 min and then an absorption spectrum of the mixture was recorded (Perkin Elmer Lambda 950 dual beam) against a blank sample (reagent solutions without carbohydrate). The absorbance of the solution was measured at two wavelengths: $\lambda_1=495$ and $\lambda_2=570$ nm and the absorbance difference ($A_{495} - A_{570}$) plotted against the concentration of the corresponding monosaccharide or disaccharide, respectively. Then, 60 μL of a selected sugar-conjugated ND particle was suspended in water (0.8 mg mL^{-1}), and treated with phenol/ H_2SO_4 and the protocol described above was applied. The concentration of conjugated sugar liberated was calculated with reference to the appropriate calibration curve. Propargyl alcohol-terminated ND particles were subjected to identical treatment and used as a blank sample.

2.5. Instrumentation

X-ray photoelectron spectroscopy: X-ray photoelectron spectroscopy (XPS) measurements were performed with an ESCALAB 220 XL spectrometer from Vacuum Generators featuring a monochromatic Al $\text{K}\alpha$ X-ray source (1486.6 eV) and a spherical energy analyzer operated in the CAE (constant analyzer energy) mode (CAE=100 eV for survey spectra and CAE = 40 eV for high-resolution spectra), using the electromagnetic lens mode. The angle between the incident X-rays and the analyzer is 58°. The detection angle of the photoelectrons is 30°.

Particle size measurements: ND suspensions (20 $\mu\text{g mL}^{-1}$) in water were sonicated. The particle size of the ND suspensions was measured at 25°C using a Zetasizer Nano ZS

(Malvern Instruments S.A., Worcestershire, U.K.) in 173° scattering geometry and the zeta potential was measured using the electrophoretic mode.

NMR measurements: ¹H (and ¹³C NMR) spectra were recorded in a 500 (125.7 for ¹³C) MHz instrument. 2D COSY, and ¹H—¹³C HMQC experiments were used to assist NMR assignments. See supporting material for spectra.

Electrospray mass spectra (ESIMS) were obtained for samples dissolved in MeCN, MeOH, or H₂O-MeOH mixtures at low μM concentrations.

Elemental analyses were performed at the Instituto de Investigaciones Químicas (Sevilla, Spain)

2.6. Biological assays:

Bacterial cell strains and eukaryotic cells

GFP-labeled *E. coli* constitutively expressing the type 1 fimbriae *fim* operon under the control of λ_{p_R} promoter (MG1655_ λ ATT::*amp_GFP_kmPcL_fimAICDFGH*) or deleted for the *fim* operon (MG1655_ λ ATT::*amp_GFP_Δfim::cat*)⁶⁷ were grown in Lysogeny Broth (LB) overnight at 37 °C at 200 rpm and diluted 1:100 to M63B1 minimal media supplemented with 0.4 % glucose (M63B1-Gluc) for another 24 h in static conditions at 37 °C. T24 human cell line derived from epithelial bladder cell (ATCC HTB-4) were grown in McCoy's 5A + Glutamax (Invitrogen) supplemented with 10 % fetal bovine serum (FBS) and maintained at 37 °C and 5 % CO₂. Cells were routinely split twice a week at a 1:5 ratio.

Yeast agglutination assay

E. coli MG1655_ λ ATT::*amp_GFP_kmPcL_fimAICDFGH* or deletion mutant MG1655_ λ ATT::*amp_GFP_Δfim::cat* were grown in M63B1-Gluc in static conditions, were washed with 1 volume of phosphate saline buffer PBS 1X twice and diluted to optical density at 600 nm (OD₆₀₀) of 1. Yeast grown in stationary phase in YPD (Yeast extract Peptone-Dextrose) were washed twice and diluted in PBS 1X. Each anti-adhesive compound was added to the bacteria sample in the quantity required to reach the desired final concentration upon mixing with yeast and the mixture incubated for 15 minutes at room temperature. Bacteria were then mixed with yeast (OD_{600nm} 1:1) and placed in a 96-well microtiter plate

and agglutination was then assessed after 10 min settling. The titer was considered as the lowest compound concentration that inhibits agglutination

Inhibition of bacterial binding to T24 bladder cells

T24 bladder cells were seeded per well into a 96-well culture plates and incubated for 24 h in the same conditions. Cell monolayer was washed three times with PBS before adding bacteria. Static bacterial cultures grown in M63B1-Gluc of the *E. coli* MG1655_λATT::amp_GFP_kmPcL_fimAICDFGH or deletion mutant MG1655_λATT::amp_GFP_Δfim::cat were washed three times with PBS and re-suspended in McCoy's 5A medium + Glutamax (Invitrogen) and vigorously vortexed in order to disperse bacterial clumps. 100 μL of bacterial suspension were then added to the cell culture, centrifuged at 100 rpm for 5 min and incubated at 37 °C in 5% CO₂. After 40 min of incubation, cells were washed twice with PBS in order to eliminate non-adherent bacteria. Attached bacteria were released with Triton X100 0.1% in PBS and transferred to a Nunclon 96 flat bottom black plates and GFP fluorescence was measured in Infinite 200 (Tecan) plate reader as a readout of bacterial load. In order to establish the multiplicity of infection for each experiment, a bacterial suspension of 1.0 OD₆₀₀ was serially diluted and used to test binding. The bacterial OD₆₀₀ used in the inhibition experiment corresponds to the amount of bacteria that allows 50% of total binding to T24 cells. Each anti-adhesive compound was added at the desired final concentration to a bacterial sample of predetermined OD₆₀₀ and the mixture incubated for 15 minutes at room temperature before the binding assay. In all cases the non fimbriated isogenic strain MG1655_λATT::amp_GFP_Δfim::cat was used as control. Experiments were performed in triplicate, at least four times, from which the corresponding IC₅₀ values were computed. The levels of fluorescence thus obtained were normalized to between 100% (MG1655_λATT::amp_GFP_kmPcL_fimAICDFGH with no compound) and 0% (MG1655_λATT::amp_GFP_Δfim::cat with no compound). Statistical analysis was performed using GraphPad Prism software.

Eukaryotic cell toxicity assay

T24 bladder cells were incubated for 24 h with each of the ND particles, serially diluted as indicated. Cell growth was determined by the MTT reduction assay (Tox-1, Sigma Inc.). Experiments were performed in triplicate at least three times. The activity in the absence of NDs was taken as 100%.

Inhibition of biofilm formation in microtiter plates

The inhibition of biofilm formation was assayed by determining the ability of the cells to adhere to the wells of 96-well non-tissue culture-treated polyvinyl chloride (PVC) microtiter dishes.⁶⁸ Overnight cultures were adjusted to OD₆₀₀ 0.05 in M63B1-Gluc medium. Compounds were serially diluted in M63B1-Gluc medium. Equal volumes of bacteria and each compound dilution were mixed, and 100 μ L aliquots of each mixture were added to a 96-well PVC plate. The plate was then incubated at 37°C for 24 h in a humid chamber. To detect biofilm formation, wells were rinsed, and 125 μ L of a 1% solution of crystal violet was added. The plates were then incubated at room temperature for 15 min and again rinsed. The crystal violet was completely dissolved by addition of 150 μ L of ethanol/acetone (80:20), and the OD₅₉₅ of the resulting solution was measured. The reported data are averages of three replicate wells in three independent experiments.

3. RESULTS AND DISCUSSION

3.1. Synthesis of trivalent sugar clusters for conjugation

Whereas conveniently functionalized peracetylated glycodendrons are often used as precursors for the generation of high-valency sugar-coated systems, in our case the presence of progargyl ester groups at the surface of the alkyne-activated “clickable” NDs prevents a post-coupling deacetylation step. Thus, the alternative fully unprotected tri- α -mannopyranosyl Man₃N₃ and tri- β -lactosyl clusters Lac₃N₃, respectively, were required (**Figure 2**). Their synthesis has been carried out by implementing a modular strategy that takes advantage of the radical addition of thiols to double bonds (ene-thiol « click » coupling) for the construction of glycodendrons.⁵⁴ The ene-thiol addition proceeds with anti-Markovnikov regioselectivity and allows the incorporation of thiosaccharidic motifs onto a polyene branching element. The resulting multivalent sugar cluster can be further armed with an azido group for subsequent conjugation purposes *via* Cu(I)-catalyzed azide-alkyne (CuAAC) coupling reaction with suitable polyalkyne partners. Readily accessible triallylated pentaerythritol **A** was chosen as the central building block.⁶⁴ The known per-*O*-acetyl-protected homo-trivalent dendrons **D**⁶² and **E**⁶³ were obtained using (i) UV light or azo-bis(isobutyronitrile) (AIBN)-initiated radical addition of either the tetra-*O*-acetyl- α -D-mannopyranose or the hepta-*O*-acetyl- β -lactose thiosugars **B** or **C**, respectively,^{65, 66} to trialkene **A**, (ii) subsequent triflyl activation of the focal primary hydroxyl in the pentaerythritol scaffold and (iii) *in situ* azide anion displacement of the thus formed triflate

derivative. Conventional catalytic deacetylation afforded the target deprotected thiosugar clusters Man_3N_3 and Lac_3N_3 , respectively (**Figure 2**). The homogeneity and purity of all new structures were confirmed by mass spectrometry, NMR spectroscopy and combustion analysis. (See supporting material for NMR and HRMS spectra).

3.2. Fabrication of sugar cluster-conjugated nanodiamonds

The precursor tri-thiomannoside (Man_3N_3) and tri-thiolactoside (Lac_3N_3) clusters were conjugated to the ND nanoparticles *via* a “click” strategy that differed from the one described for fabrication of our 1st-generation mannose-conjugated NDs (**Figure 1**).⁴⁰ In the present work, hydroxyl-terminated ND (ND-OH) was reacted with 4-pentynoic acid using *N,N'*-dicyclohexylcarbodiimide and a catalytic amount of 4-dimethylaminopyridine (DMAP) to give the corresponding ND-propargyl (**Figure 1**). The propargyl groups thus installed on the surface of the NDs were then reacted with the appropriate azido-derivatized tri-thioglycan partner (Man_3N_3 or Lac_3N_3), respectively, in the presence of $\text{CuI}(\text{PPh}_3)$ as catalyst to give the corresponding sugar cluster-clicked NDs. The successful coupling is in addition confirmed by the presence of N1s and S 2p next to C 1s and O1s in the XPS survey spectrum (**Table 1**). The initial ND-OH particles show 1.5 at % nitrogen presence most likely generated during the detonation process where trinitrotoluene is used. The level of N1s is increased in ND- Man_3 and ND- Lac_3 particles to 5.3 and 5.2 at % respectively. The S/(N-1.5) ratio is determined as 1.03 (ND- Man_3) and 0.97 (ND- Lac_3), close to the theoretical value of 1. The amount of sugar clicked to a given glyco-ND surface was quantified using a classical phenol-sulfuric acid-based colorimetric method as has been reported previously.⁴⁰ As expected (**Table 1**), the sugar loading is seen to be almost three times higher for each of the ND-tri-thioglycan clusters fabricated in this work than observed for the 1st-generation ND-sugar conjugates.⁴⁰

3.3. Inhibition of type 1 fimbriae-mediated adhesion to eukaryotic cells by mannose derivatives

Two independent assays were applied to evaluate the efficiency of the tri-thiomannoside cluster-NDs to inhibit type 1 fimbriae-mediated bacterial adhesion to eukaryotic surfaces: (i) inhibition of yeast agglutination and (ii) inhibition of bacterial adhesion on the T24 bladder cell line.

3.3.1. Yeast agglutination assay

The assay is based on measuring the capacity of *E. coli* expressing type 1 fimbriae to aggregate yeasts through bacterial recognition of mannosylated residues present on their cell surface glycans and was performed as previously described.⁴⁰ The inhibition titer was calculated as the minimum concentration of each sugar analogue or ND derivative at which agglutination was blocked. The data are summarized in **Table 2**. No inhibition of yeast aggregation was detected with either the ND-OH or tri-thiolactoside cluster-modified ND ND-Lac₃ controls. In contrast, all compounds featuring mannosyl moieties were able to inhibit the adhesion of bacteria to yeast cells to varying degrees. The ND-Man₃ particles give an inhibition titer of 3.14 μg mL⁻¹ corresponding to a potency of 2970 relative to that of methyl α-D-mannopyranoside (α-mmp), used as a monovalent reference. In comparison, a relative potency value of 1003 was obtained with our 1st-generation mannose-functionalized NDs in the same assay format.⁴⁰ The unconjugated tri-thiomannoside cluster Man₃N₃ shows a potency of 32 relative to that of α-mmp. Thus, the inhibitory potential of cluster Man₃N₃, when conjugated to the ND particles, increased 91 times more than when unconjugated.

3.3.2. Bacterial binding to T24 bladder cell inhibition assay

The new glyco-NDs were evaluated for their ability to interfere with FimH-mediated recognition by bacteria of T24 cells, a human bladder carcinoma cell line, following a previously described protocol⁴⁰ (see **Figure 3**). None of the new compounds synthesized in this work exhibited any measurable cytotoxicity towards T24 cells after 24 h of incubation at the maximum concentrations to be employed in the assay (see supplementary information **Figure S1**). As expected, neither the ND-OH, nor ND-Lac₃ controls show any tendency to inhibit adherence to T24 cells in this assay (**Table 3**). In contrast, the tri-thiomannoside cluster Man₃N₃ was found to significantly affect the adhesion, exhibiting an inhibitory potency 229-fold higher than α-mmp in this assay. The ND-Man₃ displayed an inhibition potency of 30502 relative to that of α-mmp (a value of 9259 is obtained for our 1st-generation mannose-functionalized NDs in this assay⁴⁰). The activity of the tri-thiomannoside cluster Man₃N₃ is thus seen in this assay to be amplified some 133 times when conjugated to the ND particles.

3.4. Inhibition of biofilm formation in microtiter plates

Type 1 fimbriae are well known to promote adhesion to abiotic surfaces and to enhance biofilm formation. The initial attachment and establishment of *E. coli* K-12 biofilms to

abiotic surfaces can be inhibited by α -mannopyranosyl containing *O*-glycosides and *O*-glycans, implicating the integral role of the FimH lectin in this process.⁶⁹ The biofilm disrupting ability of the various sugar ligands and conjugated-nanostructures fabricated in this work was evaluated, as previously described, using an assay that measures their ability to inhibit *E. coli* MG1655_ λ ATT::amp_GFP_kmPcL_fimAICDFGH biofilm formation on polyvinyl chloride (PVC) surfaces (**Figure 4**).⁴⁰ Whereas neither the ND-OH nor ND-Lac₃ controls proved active (data not shown), both the unconjugated tri-thiomannoside cluster Man₃N₃ and ND-Man₃ displayed a strong disrupting effect on biofilm formation as compared to α -mmp.

The biofilm inhibitory potency of the ND-Man₃ described herein is significantly greater than that observed for our 1st generation sugar-NDs (*ca.* 10 fold).⁴⁰ However, the relatively small increase in the biofilm inhibition potency of ND-Man₃N₃ relative to that of the Man₃N₃ (a factor of 2) is in sharp contrast to the large increases in adhesion inhibition observed upon conjugation of Man₃N₃ to NDs in the corresponding yeast agglutination and T24 bladder cells binding assays and perhaps deserves comment. Adhesion of bacteria to bladder cells and yeast agglutination are exclusively dependent on type 1 fimbriae, whereas biofilm formation of *E. coli* cells is known to be mediated not only by type 1 fimbriae but also through the interplay of number of additional cell surface appendages. Additionally biofilms are constituted of a complex matrix of high molecular weight constituents including polysaccharides and this would be expected to impede diffusion of large molecules such as NDs conjugates relative to that of smaller entities.

CONCLUSIONS

In this work we demonstrate that sugar-conjugated nanodiamonds have marked detrimental effects on *E. coli*-mediated biofilm formation and that this phenomenon is related to their ability to interfere with FimH-mediated bacterial adhesion. The conjugation strategy developed for these 2nd-generation sugar conjugated NDs, using alkynyl-functionalized NDs, proves as efficient as the one described previously which was based on azido-functionalized NDs.⁴⁰ Having in hand this pair of complementary strategies for surface modification of ND particles, makes possible the application of the Huisgen Cu(I) “click” methodology to a wide range of propargyl- or azido-armed ligand counterparts thus greatly broadening its scope. The demonstration that the tri-thiomannoside cluster-NDs (ND-Man₃) fabricated here are able to effectively impede type 1 fimbriae-mediated bacterial adhesion in two independent assay

formats is consistent with our earlier findings that mannose-conjugated NDs have a marked *E.coli* anti-adhesive activity.

The ability of the new glycocluster-NDs to significantly inhibit *E. coli*-mediated biofilm formation is remarkable. The fact that both the 1st-(glycoside) and 2nd-(thioglycoside) generations of glyco-NDs both manifest this property is also notable.⁴⁰ Moreover, the finding that the unconjugated trimeric thiomannoside cluster Man₃N₃ shows a non-negligible activity as a biofilm inhibitor, despite its low relative molecular weight was unexpected. Indeed, rarely have sugar-based inhibitors of *E. coli*-generated biofilms been reported although a number have for biofilms mediated by *Pseudomonas aeruginosa*.^{70, 71} The fact that Man₃N₃ does not feature any triazole segment in the vicinity of the sugar moiety strongly suggests that the presence of the heterocycle as an integral feature of the 1st-generation NDs is not critical for their ability to inhibit biofilm formation. In addition, neither the ND-OH nor ND-Lac₃ controls are seen to show any anti-adhesive activity, underlining that the activities observed for the thiomannosyl conjugates are sugar-specific. Taken together, the data supports that it is the presence of mannosyl residues in the thiosugar clusters that constitute the primary ingredient driving the biofilm-inhibitory activity observed for the ND-conjugates: neither the presence of triazole functions or the interplay of some intrinsic physico-chemical property of the nanodiamond core itself have an obvious influence on this process.

Although it would be premature to advance a detailed explanation for this observation at this point, such biofilm inhibition effects would constitute a useful additional feature of any anti-adhesive lead and has rarely been reported in the past for the alternative mono- or multivalent- mannose derivatives. We suspect that the activities brought to light in this work might not be exclusive to nanodiamond-based sugar conjugates. Moreover, the finding that the tri-thiomannosyl cluster Man₃N₃ itself is a relatively efficient inhibitor, even when not conjugated to any ND scaffold, suggests that alternative mono- and medium- to low-valency mannosyl conjugates might also demonstrate significant *E. coli*-mediated biofilm disrupting properties, a hypothesis that deserves to be further investigated

ACKNOWLEDGEMENTS

A.B, M.K., R.B and S.S. gratefully acknowledge financial support from the Centre National de Recherche Scientifique (CNRS), the Université Lille 1, the Nord Pas de Calais region and the Institut Universitaire de France (IUF). A.S. gratefully acknowledges financial support

from the CNRS and the IFCPAR (Indo-French Centre for the Promotion of Advanced Research) (Project 3905-1) and the Region Picardie for a doctoral fellowship to J.-S. Baumann. F. L. is supported by a MENESR (Ministère Français de l'Éducation Nationale, de l'Enseignement Supérieur et de la Recherche) fellowship. C.B. and J-M.G. are supported by the Institut Pasteur, the French Government's Investissement d'Avenir program Laboratoire d'Excellence "Integrative Biology of Emerging Infectious Diseases" (grant n°ANR-10-LABX-62-IBEID) and from Fondation pour la Recherche Médicale grant "Equipe FRM DEQ20140329508". C.O.M. and J.M.G.F. are grateful to the Spanish Ministerio de Economía y Competitividad (contract numbers SAF2013-44021-R and CTQ2010-15848), the Junta de Andalucía (contract number FQM2012 1467) and the European Regional Development Funds (FEDER and FSE) for financial support. We also acknowledge support from the European Union through the FP7-PEOPLE-2010-IRSES action "Photorelease" (grant number 269099) and the COST action CM1102 "MultiGlycoNano".

REFERENCES

- 1 N. Hoiby, O. Ciofu, H.K. Johansen, Z.J. Song, C. Moser, P.O. Jensen, S. Molin, M. Givskov, T. Tolker-Nielsen, T. Bjarnsholt, *Int J Oral Sci*, 2011, **3** 55-65.
- 2 D. Lebeaux, A. Chauhan, O. Rendueles, C. Beloin, *Pathogens*, 2013, **2** 288-356.
- 3 G. O'Toole, H.B. Kaplan, R. Kolter, *Annual review of microbiology*, 2000, **54** 49-79.
- 4 N. Hoiby, T. Bjarnsholt, M. Givskov, S. Molin, O. Ciofu, *Int J Antimicrob Agents*, 2010, **35** 322-332.
- 5 D. Lebeaux, J.M. Ghigo, C. Beloin, *Microbiol Mol Biol Rev*, 2014, **78** 510-543.
- 6 A. Chauhan, A. Bernardin, W. Mussard, I. Kriegel, M. Esteve, J.M. Ghigo, C. Beloin, V. Semetey, *J Infect Dis*, 2014, **210** 1347-56.
- 7 O. Rendueles, J.B. Kaplan, J.M. Ghigo, *Environ Microbiol*, 2013, **15** 334-346.
- 8 L.R. Rodrigues, *Adv Exp Med Biol*, 2011, **715** 351-367.
- 9 C.K. Cusumano, J.S. Pinkner, Z. Han, S.E. Greene, B.A. Ford, J.R. Crowley, J.P. Henderson, J.W. Janetka, S.J. Hultgren, *Sci Transl Med*, 2011, **3** 109ra115.
- 10 A.M. Krachler, K. Orth, *Virulence*, 2013, **4** 284-294.
- 11 D. Romero, E. Sanabria-Valentin, H. Vlamakis, R. Kolter, *Chem Biol*, 2013, **20** 102-110.
- 12 N. Sharon, *Biochim Biophys Acta*, 2006, **1760** 527-537.
- 13 M. Totsika, M. Kostakioti, T.J. Hannan, M. Upton, S.A. Beatson, J.W. Janetka, S.J. Hultgren, M.A. Schembri, *J Infect Dis*, 2013, **208** 921-928.
- 14 R.P. Allaker, K. Memarzadeh, *Int J Antimicrob Agents*, 2014, **43** 95-104.
- 15 S. Chernousova, M. Epple, *Angew Chem Int Ed Engl*, 2013, **52** 1636-1653.
- 16 M.R. Das, R.K. Sarma, S. Borah, R. Kumari, R. Saikia, A.B. Deshmukh, M.V. Shelke, P. Sengupta, S. Szunerits, R. Boukherroub, *Colloids Surf B Biointerfaces*, 2013, **105** 128-136.
- 17 I. Francolini, G. Donelli, *FEMS Immunol Med Microbiol*, 2010, **59** 227-238.
- 18 A. Herman, A.P. Herman, *J Nanosci Nanotechnol*, 2014, **14** 946-957.
- 19 E. Taylor, T.J. Webster, *Int J Nanomedicine*, 2011, **6** 1463-1473.
- 20 M. Hartmann, T.K. Lindhorst, *Eur J Org Chem*, 2011, 3583-3609.
- 21 P. Klemm, M. Schembri, Type 1 Fimbriae, Curli, and Antigen 43: Adhesion, Colonization, and Biofilm Formation, in: A. Böck, R. Curtiss III, J.B. Kaper, F.C. Neidhardt, T. Nyström, K.E. Rudd, C.L. Squires (Eds.) *EcoSal- Escherichia coli and Salmonella: cellular and molecular biology*, ASM Press, Washington, D.C., 2004.
- 22 X.R. Wu, T.T. Sun, J.J. Medina, *Proc Natl Acad Sci U S A*, 1996, **93** 9630-9635.
- 23 N. Jayaraman, *Chem Soc Rev*, 2009, **38** 3463-3483.
- 24 I. Ofek, D.L. Hasty, N. Sharon, *FEMS Immunol Med Microbiol*, 2003, **38** 181-191.
- 25 S. Brument, A. Sivignon, T.I. Dumych, N. Moreau, G. Roos, Y. Guerardel, T. Chalopin, D. Deniaud, R.O. Bilyy, A. Darfeuille-Michaud, J. Bouckaert, S.G. Gouin, *J Med Chem*, 2013, **56** 5395-5406.
- 26 Z. Han, J.S. Pinkner, B. Ford, E. Chorell, J.M. Crowley, C.K. Cusumano, S. Campbell, J.P. Henderson, S.J. Hultgren, J.W. Janetka, *J Med Chem*, 2012, **55** 3945-3959.
- 27 X. Jiang, D. Abgottspon, S. Kleeb, S. Rabbani, M. Scharenberg, M. Wittwer, M. Haug, O. Schwardt, B. Ernst, *J Med Chem*, 2012, **55** 4700-4713.
- 28 N. Nagahori, R.T. Lee, S. Nishimura, D. Page, R. Roy, Y.C. Lee, *Chembiochem*, 2002, **3** 836-844.
- 29 A. Patel, T.K. Lindhorst, *Carbohydr Res*, 2006, **341** 1657-1668.
- 30 R.J. Pieters, *Org Biomol Chem*, 2009, **7** 2013-2025.
- 31 M. Touaibia, A. Wellens, T.C. Shiao, Q. Wang, S. Sirois, J. Bouckaert, R. Roy, *ChemMedChem*, 2007, **2** 1190-1201.
- 32 L.L. Kiessling, J.E. Gestwicki, L.E. Strong, *Curr Opin Chem Biol*, 2000, **4** 696-703.
- 33 C.C. Lin, Y.C. Yeh, C.Y. Yang, C.L. Chen, G.F. Chen, C.C. Chen, Y.C. Wu, *J Am Chem Soc*, 2002, **124** 3508-3509.

- 34 J.J. Lundquist, E.J. Toone, *Chem Rev*, 2002, **102** 555-578.
- 35 M. Mammen, S.-K. Choi, G.M. Whitesides, *Angew. Chem. Int. Ed.*, 1998, **37** 2754-2899.
- 36 M. Durka, K. Buffet, J. Iehl, M. Holler, J.F. Nierengarten, J. Taganna, J. Bouckaert, S.P. Vincent, *Chem Commun (Camb)*, 2011, **47** 1321-1323.
- 37 Y.C. Lee, R.T. Lee, *Acc. Chem. Res.*, 1995, **28** 321-327.
- 38 A. Bernardi, J. Jimenez-Barbero, A. Casnati, C. De Castro, T. Darbre, F. Fieschi, J. Finne, H. Funken, K.E. Jaeger, M. Lahmann, T.K. Lindhorst, M. Marradi, P. Messner, A. Molinaro, P.V. Murphy, C. Nativi, S. Oscarson, S. Penades, F. Peri, R.J. Pieters, O. Renaudet, J.L. Reymond, B. Richichi, J. Rojo, F. Sansone, C. Schaffer, W.B. Turnbull, T. Velasco-Torrijos, S. Vidal, S. Vincent, T. Wennekes, H. Zuilhof, A. Imberty, *Chem Soc Rev*, 2013, **42** 4709-4727.
- 39 M.A. Mintzer, E.L. Dane, G.A. O'Toole, M.W. Grinstaff, *Mol Pharm*, 2012, **9** 342-354.
- 40 A. Barras, F.A. Martin, O. Bande, J.S. Baumann, J.M. Ghigo, R. Boukherroub, C. Beloin, A. Siriwardena, S. Szunerits, *Nanoscale*, 2013, **5** 2307-2316.
- 41 M. Hartmann, P. Betz, Y. Sun, S.N. Gorb, T.K. Lindhorst, A. Krueger, *Chemistry*, 2012, **18** 6485-6492.
- 42 A. Siriwardena, A. Barras, F.A. Martin, O. Bande, J.S. Baumann, J.M. Ghigo, C. Beloin, R. Boukherroub, S. Szunerits, *Glycoconj. J.*, 2011, **28** 216.
- 43 A. Barras, J. Lyskawa, S. Szunerits, P. Woisel, R. Boukherroub, *Langmuir*, 2011, **27** 12451-12457.
- 44 A. Barras, S. Szunerits, L. Marcon, N. Monfilliette-Dupont, R. Boukherroub, *Langmuir*, 2010, **26** 13168-13172.
- 45 Y.R. Chang, H.Y. Lee, K. Chen, C.C. Chang, D.S. Tsai, C.C. Fu, T.S. Lim, Y.K. Tzeng, C.Y. Fang, C.C. Han, H.C. Chang, W. Fann, *Nat Nanotechnol*, 2008, **3** 284-288.
- 46 S.A. Dahoumane, M.N. Nguyen, A. Thorel, J.P. Boudou, M.M. Chehimi, C. Mangeney, *Langmuir*, 2009, **25** 9633-9638.
- 47 A. Krüger, *Angew. Chem. Int. Ed.*, 2006, **45** 6426-6427.
- 48 A. Krüger, *Chemistry*, 2008, **14** 1382-1390.
- 49 Y. Liang, M. Ozawa, A. Krueger, *ACS Nano*, 2009, **3** 2288-2296.
- 50 V.N. Mochalin, O. Shenderova, D. Ho, Y. Gogotsi, *Nat Nanotechnol*, 2012, **7** 11-23.
- 51 L. Marcon, F. Riquet, D. Vicogne, S. Szunerits, J.-F. Bodart, R. Boukherroub, *J. Mater. Chem.*, 2010, **20** 8064-8069.
- 52 K.-K. Liu, C.-L. Cheng, C.C. Chang, J.-I. Chao, *Nanotech.*, 2007, **18** 325102.
- 53 A.M. Schrand, H. Huang, C. Carlson, J.J. Schlager, E. Omacr Sawa, S.M. Hussain, L. Dai, *J Phys Chem B*, 2007, **111** 2-7.
- 54 S.J. Yu, M.W. Kang, H.C. Chang, K.M. Chen, Y.C. Yu, *J Am Chem Soc*, 2005, **127** 17604-17605.
- 55 A. Wellens, C. Garofalo, H. Nguyen, N. Van Gerven, R. Slattegard, J.P. Hernalsteens, L. Wyns, S. Oscarson, H. De Greve, S. Hultgren, J. Bouckaert, *PLoS One*, 2008, **3** e2040.
- 56 J.M. Benito, M. Gomez-Garcia, C. Ortiz Mellet, I. Baussanne, J. Defaye, J.M. Garcia Fernandez, *J Am Chem Soc*, 2004, **126** 10355-10363.
- 57 J.L. Jimenez Blanco, C. Ortiz Mellet, J.M. Garcia Fernandez, *Chem Soc Rev*, 2013, **42** 4518-4531.
- 58 A. Martinez, C. Ortiz Mellet, J.M. Garcia Fernandez, *Chem Soc Rev*, 2013, **42** 4746-4773.
- 59 J. Rodriguez-Lavado, M. de la Mata, J.L. Jimenez-Blanco, M.I. Garcia-Moreno, J.M. Benito, A. Diaz-Quintana, J.A. Sanchez-Alcazar, K. Higaki, E. Nanba, K. Ohno, Y. Suzuki, C. Ortiz Mellet, J.M. Garcia Fernandez, *Org Biomol Chem*, 2014, **12** 2289-2301.
- 60 K.H. Schlick, J.R. Morgan, J.J. Weiel, M.S. Kelsey, M.J. Cloninger, *Bioorg Med Chem Lett*, 2011, **21** 5078-5083.

- 61 M. Gingras, Y.M. Chabre, M. Roy, R. Roy, *Chem Soc Rev*, 2013, **42** 4823-4841.
- 62 M. Gomez-Garcia, J.M. Benito, R. Gutierrez-Gallego, A. Maestre, C.O. Mellet, J.M. Fernandez, J.L. Blanco, *Org Biomol Chem*, 2010, **8** 1849-1860.
- 63 M. Gomez-Garcia, J.M. Benito, A.P. Butera, C. Ortiz Mellet, J.M. Garcia Fernandez, J.L. Jimenez Blanco, *J Org Chem*, 2012, **77** 1273-1288.
- 64 A. Lubineau, A. Malleron, C. Le Narvor, *Tetrahedron Lett.*, 2000, **41** 8887-8891.
- 65 D.A. Fulton, J.F. Stoddart, *J Org Chem*, 2001, **66** 8309-8319.
- 66 K.L. Matta, R.N. Girotra, J.J. Barlow, *Carbohydr Res*, 1975, **43** 101-109.
- 67 C.G. Korea, R. Badouraly, M.C. Prevost, J.M. Ghigo, C. Beloin, *Environ Microbiol*, 2010, **12** 1957-1977.
- 68 A. Roux, C. Beloin, J.M. Ghigo, *J Bacteriol*, 2005, **187** 1001-1013.
- 69 L.A. Pratt, R. Kolter, *Mol Microbiol*, 1998, **30** 285-293.
- 70 J.L. Reymond, M. Bergmann, T. Darbre, *Chem Soc Rev*, 2013, **42** 4814-4822.
- 71 E.L. Dane, A.E. Ballok, G.A. O'Toole, M.W. Grinstaff, *Chem Sci*, 2014, **5** doi: 10.1039/C3SC52777H.

Table 1: Selected physical properties of the sugar-conjugated NDs

	Diameter (nm)	PI ^a	Zeta potential (mV)	Sugar loading ($\mu\text{g mg}^{-1}$ ND)	N 1s at. %	S 2p at. %
ND-OH	89 \pm 13	0.246 \pm 0.002	35.3 \pm 1.6	-	1.5	-
ND-alkynyl	126 \pm 3	0.168 \pm 0.021	34.2 \pm 1.4	-	1.5	-
ND-Man ₃	125 \pm 9	0.345 \pm 0.003	27.2 \pm 0.5	168 \pm 12	5.3	3.9
ND-Lac ₃	138 \pm 8	0.258 \pm 0.062	31.2 \pm 0.4	135 \pm 18	5.2	3.6

^a Polydispersity Index; mean \pm SD, n = 3

1

Table 2: Inhibition of type 1 fimbriae-mediated yeast agglutination

Compound	IT ($\mu\text{g mL}^{-1}$) ^a	RIT (μM) ^b	RIP ₅₀ (RIC ₅₀ α -mmp/ RIC ₅₀ of the compound)	RIP ₅₀ (RIC ₅₀ (Man ₃ N ₃)/RIC ₅₀ of the compound)
α -mmp	-	7000	1	
Man ₃ N ₃	63.4	218.8	32	
ND-Man ₃	3.14	2.4	2970	91
ND-Lac ₃	>100	^c	-	
ND-OH	>100	^c	-	
ND-mannose ^d	19.4	6.98	1003	

^a IT= inhibition titre, ^bRIT= relative inhibition titre= IT \times 3.45 μmol mannose/mg for Man₃N₃ or 0.75 μmol mannose/mg for ND-Man₃ or 0.49 μmol lactose/mg for ND-Lac₃, RIP₅₀= relative inhibition potency of either α -mmp or Man₃N₃/RIC₅₀ of the corresponding ND-conjugate. All relative inhibition parameters are expressed as micromolar concentration of carbohydrate.

^c Values not determined. Sigmoidal fitting of data not possible.

^d These parameters correspond to those reported for 1st-generation mannose-NDs.⁴⁰

Table 3: Inhibition of type 1 fimbriae mediated adhesion to T24 bladder cells

Compound	IC ₅₀ ($\mu\text{g mL}^{-1}$)	RIC ₅₀ (μM) ^a	RIP ₅₀ (RIC ₅₀ α -mmp/ RIC ₅₀ of the compound)	RIP ₅₀ (RIC ₅₀ (Man ₃ N ₃)/RIC ₅₀ of the compound)
α -mmp	-	22511	1	
Man ₃ N ₃	28.5	98.2	229	
ND-Man ₃	0.98	0.738	30502	133
ND- Lac ₃	>100	^b		
ND-OH	>100	^b		
ND-mannose ^c	7.6	2.7	9259	

^a RIC₅₀= relative IC₅₀ = IC₅₀ \times 3.45 μmol mannose/mg for Man₃N₃ or 0.75 μmol mannose/mg for ND-Man₃ or 0.49 μmol lactose/mg for ND-Lac₃, RIP₅₀= relative inhibition potency of α -mmp or Man₃N₃/RIC₅₀ of the compound. All relative inhibition parameters are expressed as micromolar concentration of carbohydrate.

^b Values not determined. Sigmoidal fitting of data not possible.

^c These parameters correspond to those reported for 1st-generation mannose-NDs.⁴⁰

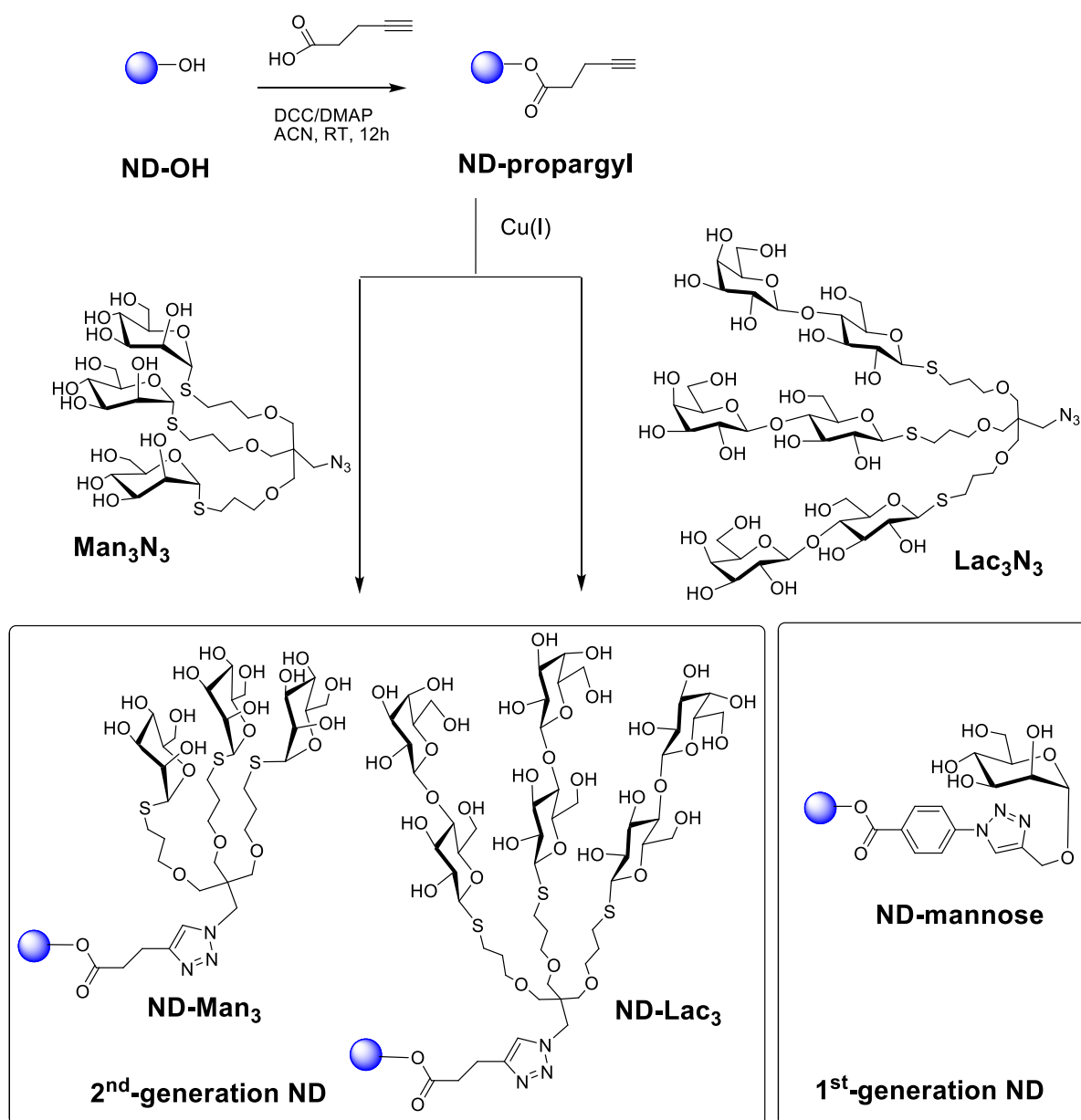


Figure 1. Schematic illustration of the stepwise chemical functionalization of diamond nanoparticles (ND) to give the target ND-conjugated trimeric thiosugar clusters (2nd-generation ND). For comparison, the structure of the 1st-generation ND (ND-mannose)⁴⁰ is presented.

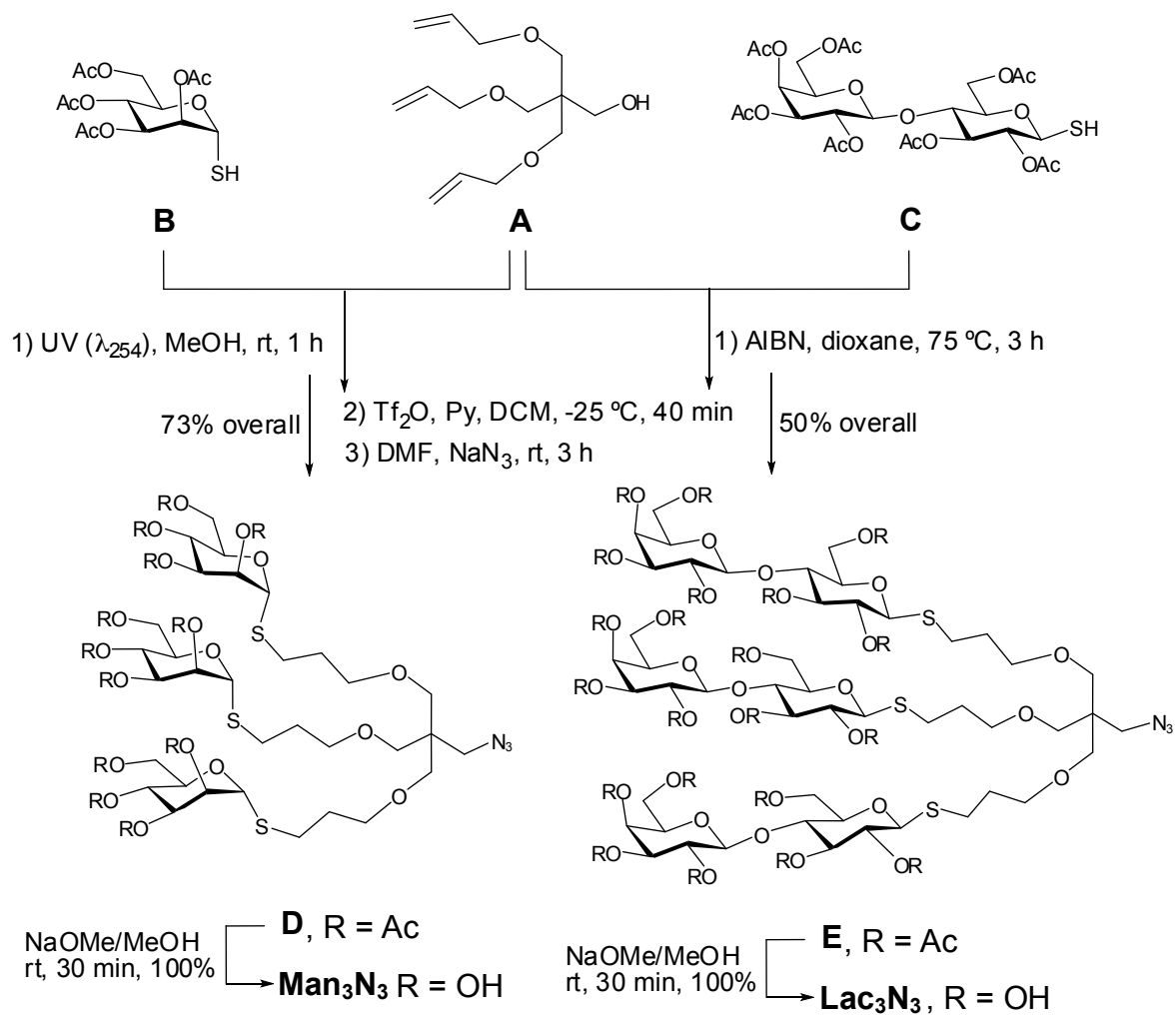


Figure 2. Synthetic routes to tri-thiomannoside Man_3N_3 and tri-thiolactoside Lac_3N_3 clusters.

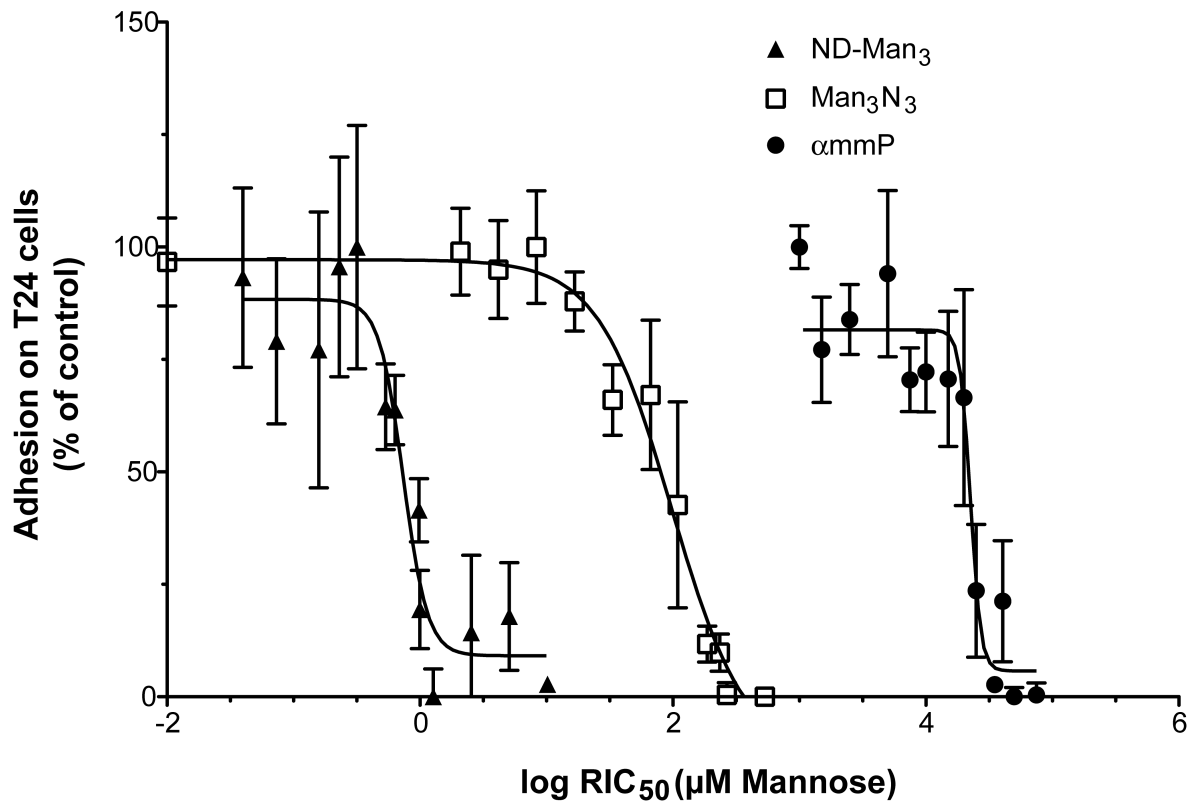


Figure 3. Inhibitory effects of mannosylated compounds on type 1 fimbriae-mediated adhesion to T24 bladder epithelial cells. *E. coli* MG1655_λATT::amp_GFP_kmPcL_fimAICDFGH or deletion mutant MG1655_λATT::amp_GFP_Δfim::cat were mixed with the various compounds individually added and incubated with T24 bladder cells for 40 min. After washing, adhesion was evaluated by measurements of gfp fluorescence using a Tecan Sunrise™ multiwell plate reader and expressed as relative fluorescence units (R.F.U.). The fluorescence values thus obtained were normalized to between 100% (MG1655_λATT::amp_GFP_kmPcL_fimAICDFGH with no compound) and 0% (MG1655_λATT::amp_GFP_Δfim::cat with no compound). Data are expressed as the percentage of bacteria adhered with respect to that in the absence of compound. Experiments were performed in triplicate at least twice. Determination of IC₅₀ values were performed with GraphPad Prism software (GraphPad Inc.). Sigmoidal fitting curves of the log of Relative Inhibitory Concentration 50 (RIC₅₀) are represented for α-mmp, tri-thiomannoside cluster, Man₃N₃ and ND-Man₃.

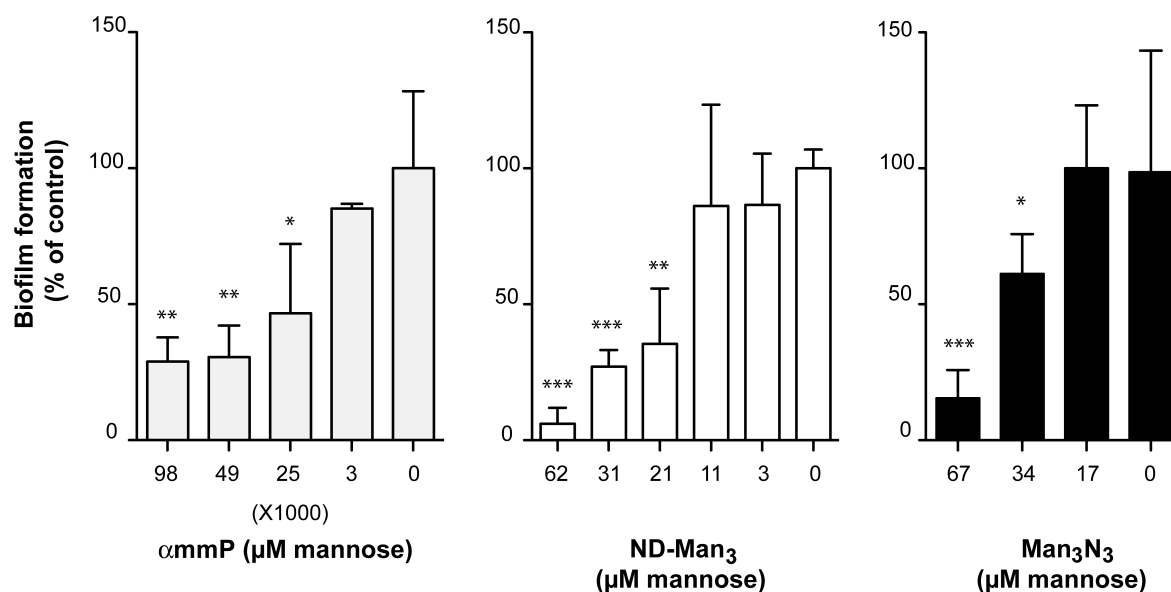


Figure 4. Inhibitory effects of mannosylated compounds on type 1 fimbriae-mediated biofilm formation. The various compounds were individually added at the start of biofilm growth in increasing particles concentration within microtiter plates. After 24 h of growth at 37°C in M63B1-Gluc media, biofilm formation was evaluated using crystal violet staining. Experiments were performed in triplicate at least twice. Crystal violet measurements were performed in a Tecan Sunrise™ multiwell plate reader. Adhesion was set do 100% in absence of compounds. Data are expressed as the percentage of adhesion of bacteria with respect to that in the absence of compound. Bars represents mean +/- SD, n= 3. Statistical differences were evaluated using one-way ANOVA included in Graphpad Prism Version 5.0c. *p < 0.05, **p < 0.01, ***p < 0.001.